

Black hole accretion

Feng Yuan (袁 峰)

Shanghai Astronomical Observatory
Chinese Academy of Sciences

Outline

- Chapter 1: Introduction to some basic concepts and Review of accretion models
- Chapter 2: The standard thin disk and slim disk
- Chapter 3: Hot accretion flow: dynamics & radiation
- Chapter 4: Hot accretion flow: applications
- Chapter 5: Wind and jet
- Chapter 6: AGN feedback

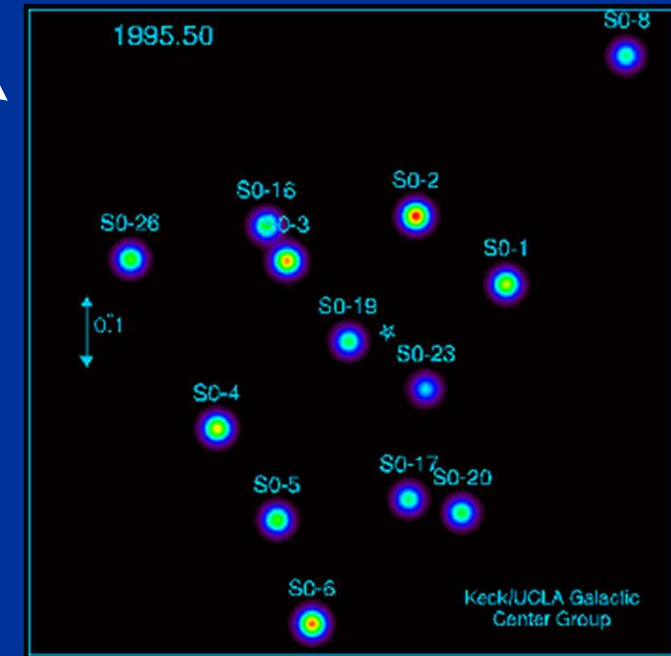
Chapter 4:

Applications in Sgr A* & LLAGNs

4.1 Accretion onto Sgr A*

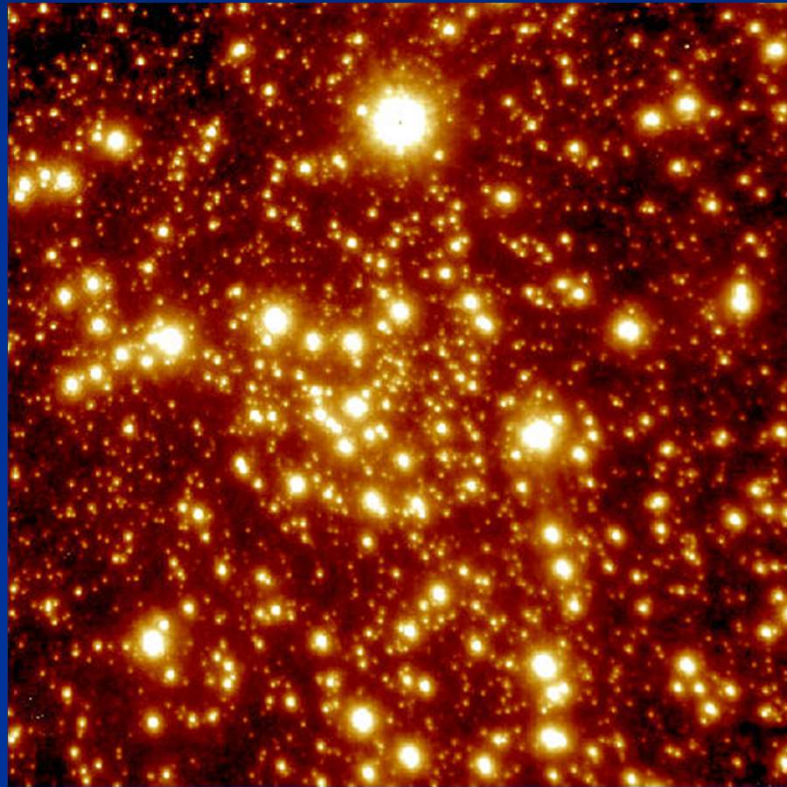
Why Sgr A* so interesting?

- Best evidence for a BH (stellar orbits)
 - $M \approx 4 \times 10^6 M_{\odot}$
- Largest BH on the sky (horizon $\approx 8 \mu''$), thus most detailed constraints on ambient conditions around BH
 - Direct observational determination to the accretion rate
 - Outer boundary conditions
- Abundant observational data:
 - Detailed SED
 - polarization
 - X-ray & IR flares probe gas at $\sim R_s$
 - emission lines
- Accretion physics at extreme low luminosity ($L \sim 10^{-9} L_{\text{EDD}}$), useful and unique laboratory for low-luminosity AGNs!



Fuel Supply

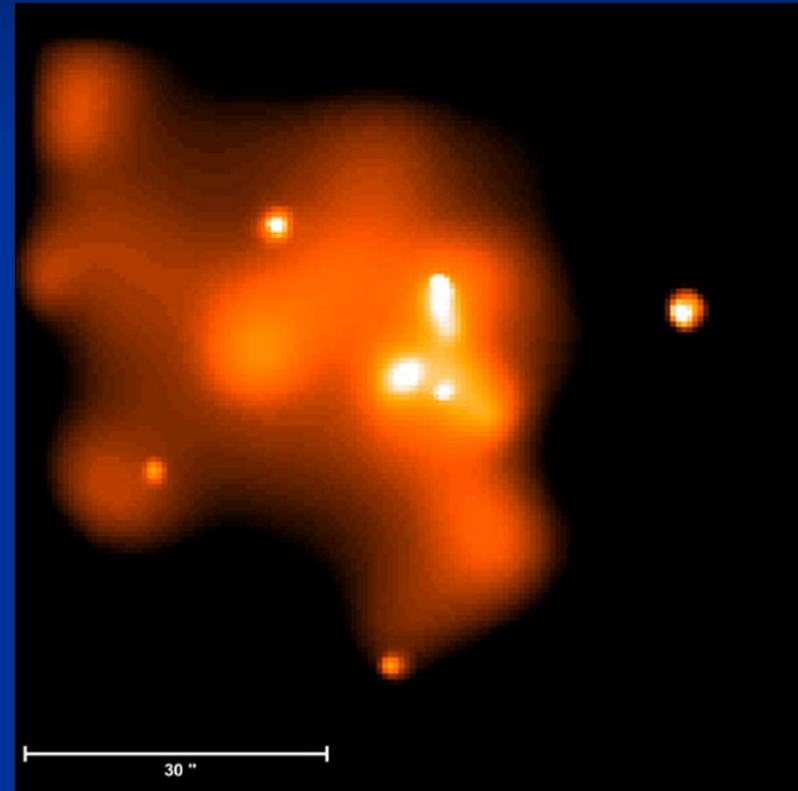
IR (VLT) image of central \sim pc



Genzel et al. 2003, Nature

Young cluster of massive stars
in the central \sim pc loses $\sim 10^{-3}$
 $M_{\odot} \text{ yr}^{-1}$ ($\approx 2-10''$ from BH)

Chandra image of central ~ 3 pc



Baganoff et al. 2003, ApJ

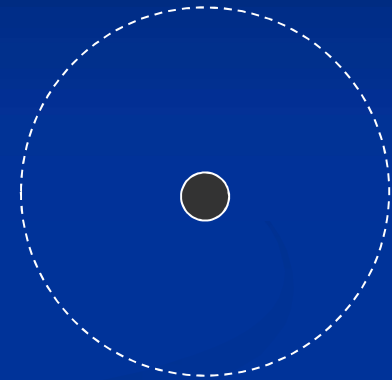
Hot x-ray emitting gas
($T = 1-2 \text{ keV}$; $n = 100 \text{ cm}^{-3}$)
produced via shocked
stellar winds

Outer Boundary Conditions at Bondi Radius

- **Temperature:** 2keV; **Density:** 130cm^{-3}

- **Bondi radius:**

$$R_A \approx \frac{GM}{c_s^2} \approx 1'' \approx 10^5 R_s$$



- **Mass accretion rate estimation**

$$\dot{M}_{\text{captured}} \approx 4\pi R_A^2 \rho c_s \Big|_{R \approx R_A} \approx 10^{-5} M_{\odot} \text{yr}^{-1}$$

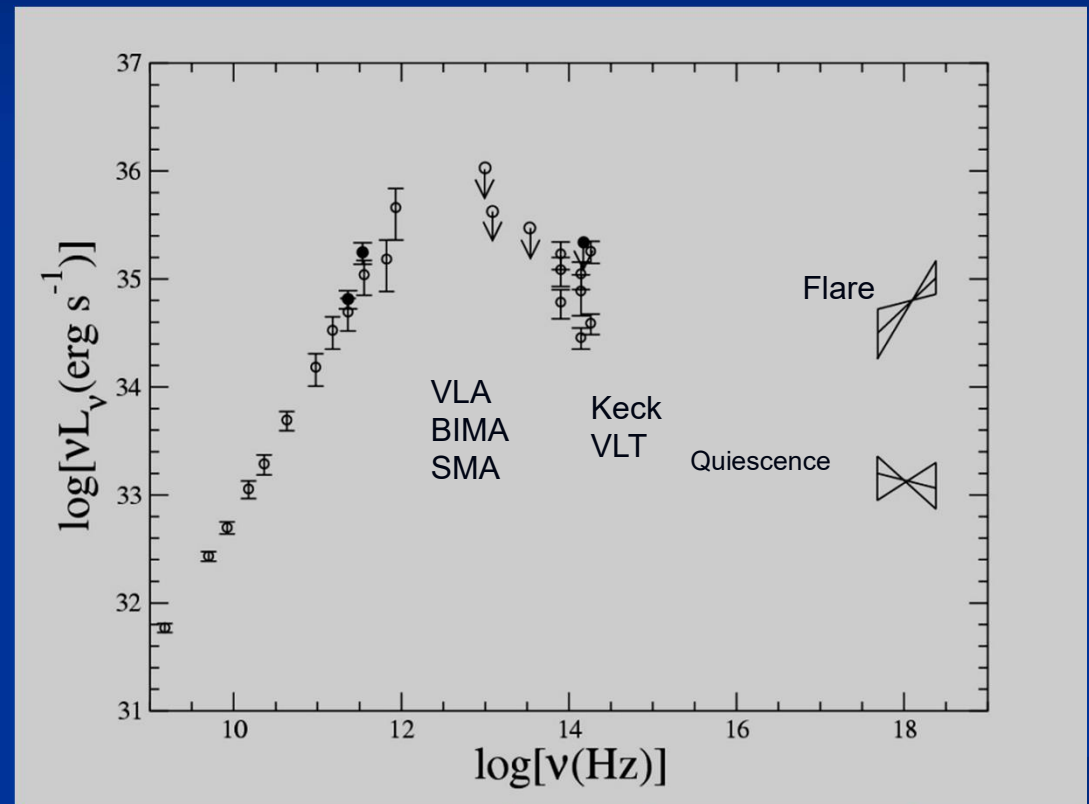
this is roughly consistent with the numerical simulation of Cuadra et al. (2006, MNRAS):

$$\dot{M} \approx 3 \times 10^{-6} M_{\odot} \text{yr}^{-1}$$

- **Angular momentum:** quite large, the circularization radius $\sim 10^4 R_s$, not a spherical accretion (Cuadra et al. 2006)

Observational results for Sgr A* (I): Spectrum

- flat radio spectrum
- submm-bump
- two X-ray states
 - quiescent: photon indx=2.2
 - flare: photon index=1.3
- Total Luminosity $\sim 10^{36}$ ergs s⁻¹
 $\sim 100 L_{\odot} \sim 10^{-9} L_{\text{EDD}} \sim 10^{-6} \dot{M} c^2$



“Old” ADAF Model for Sgr A*

- The “old” ADAF (e.g., Ichimaru 1977; Rees et al. 1982; Narayan & Yi 1994;1995; Abramowicz et al. 1995...)
 - Key idea: energy advection
 - Accretion rate is constant of radius
- Success of this ADAF model (Narayan et al. 1995, Nature; Narayan et al. 1998):
 - low luminosity of Sgr A*;
 - rough fitting of SED;

However:

- New radio polarization observations find strong LP (Aitken et al. 2001; Bower et al. 2003, 2005)
- Conflict with the prediction of ADAF:
 - Due to strong Faraday depolarization effect

Observational constraint: Polarization

Aitken et al. 2001; Bower et al. 2003; 2005; Marrone et al. 2007...

- At cm wavelength: no LP but strong CP;
- at submm-bump:
 - high LP: (5-10)% at 230 & 340 GHz; <2% at 112 GHz
- a strict constraint to density & B field:

RM (Faraday rotation measure) can not be too large:

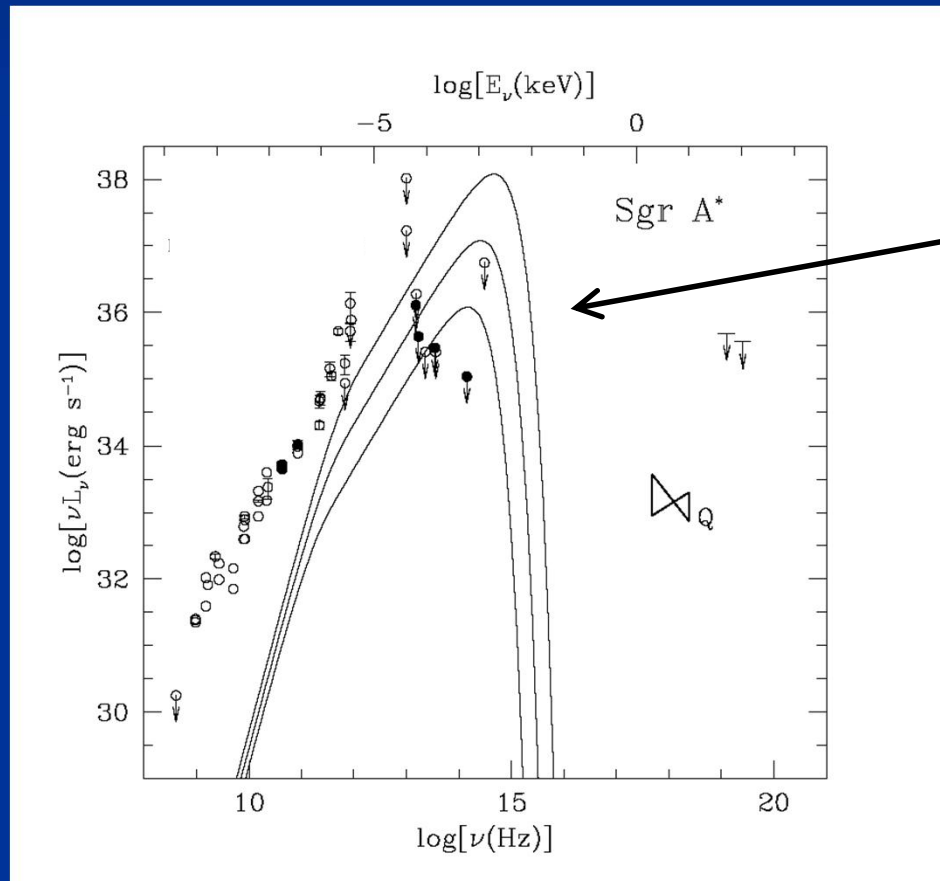
$$RM = 8.1 \times 10^5 \int n_e \vec{B} \cdot \hat{r} dr \leq 2 \times 10^5 \text{ rad m}^{-2}$$

- Constraints on accretion rate at the innermost region:

$$2 \times 10^{-9} M_{\odot} \text{ yr}^{-1} < \dot{M} < 2 \times 10^{-7} M_{\odot} \text{ yr}^{-1}$$

So accretion rate decreases inward ---- see lecture on wind production

The Standard Thin Disk Ruled Out



1. inferred low efficiency

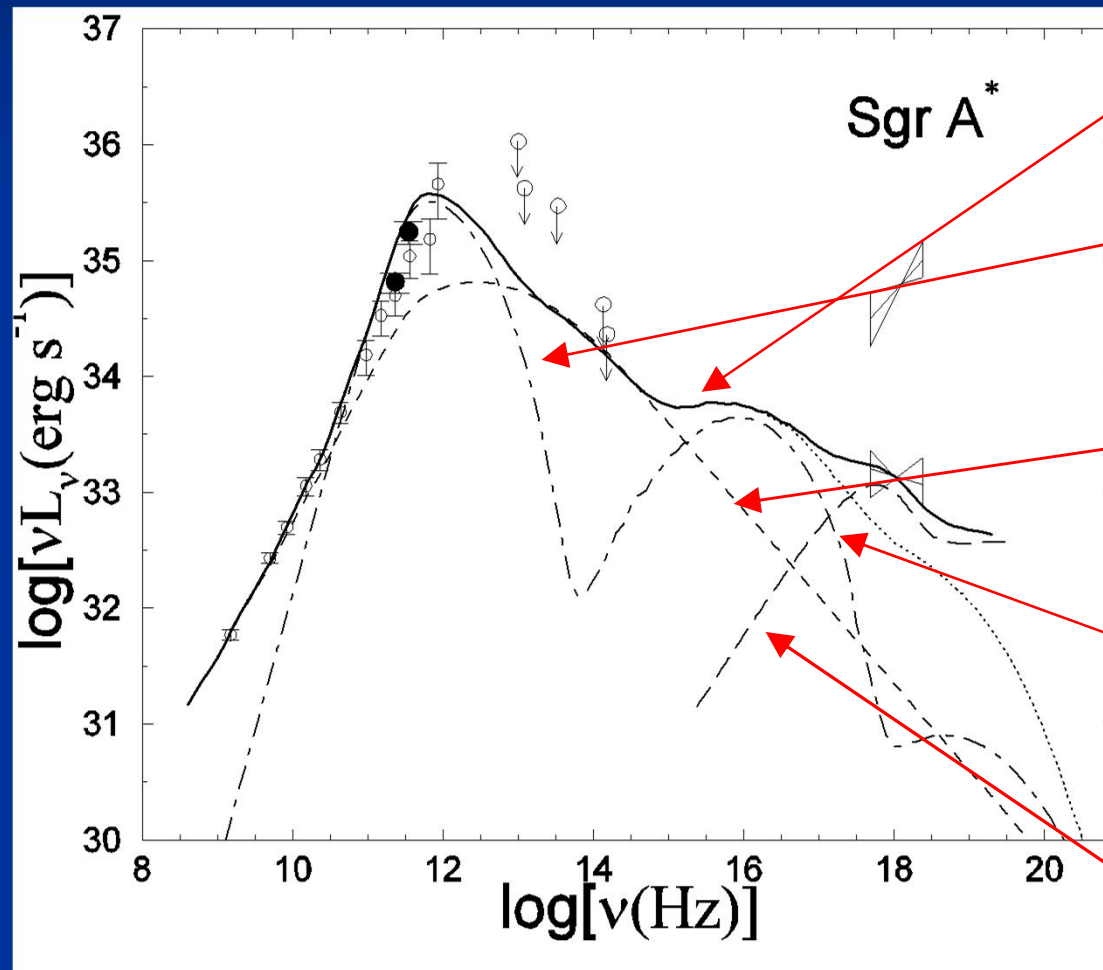
2. where is the expected blackbody emission?

$$\dot{M}_{\text{disk}} < 10^{-10} M_{\odot} \text{yr}^{-1}$$

3. observed gas on $\sim 1''$ scales is primarily hot & spherical, not disk-like

4. absence of stellar eclipses argues against $\tau \gg 1$ disk
(Cuadra et al. 2003)

ADAF (RIAF) model of quiescent state of Sgr A*



Total emission

Synchrotron emission (from thermal electrons)

synchrotron emission (from power-law electrons)

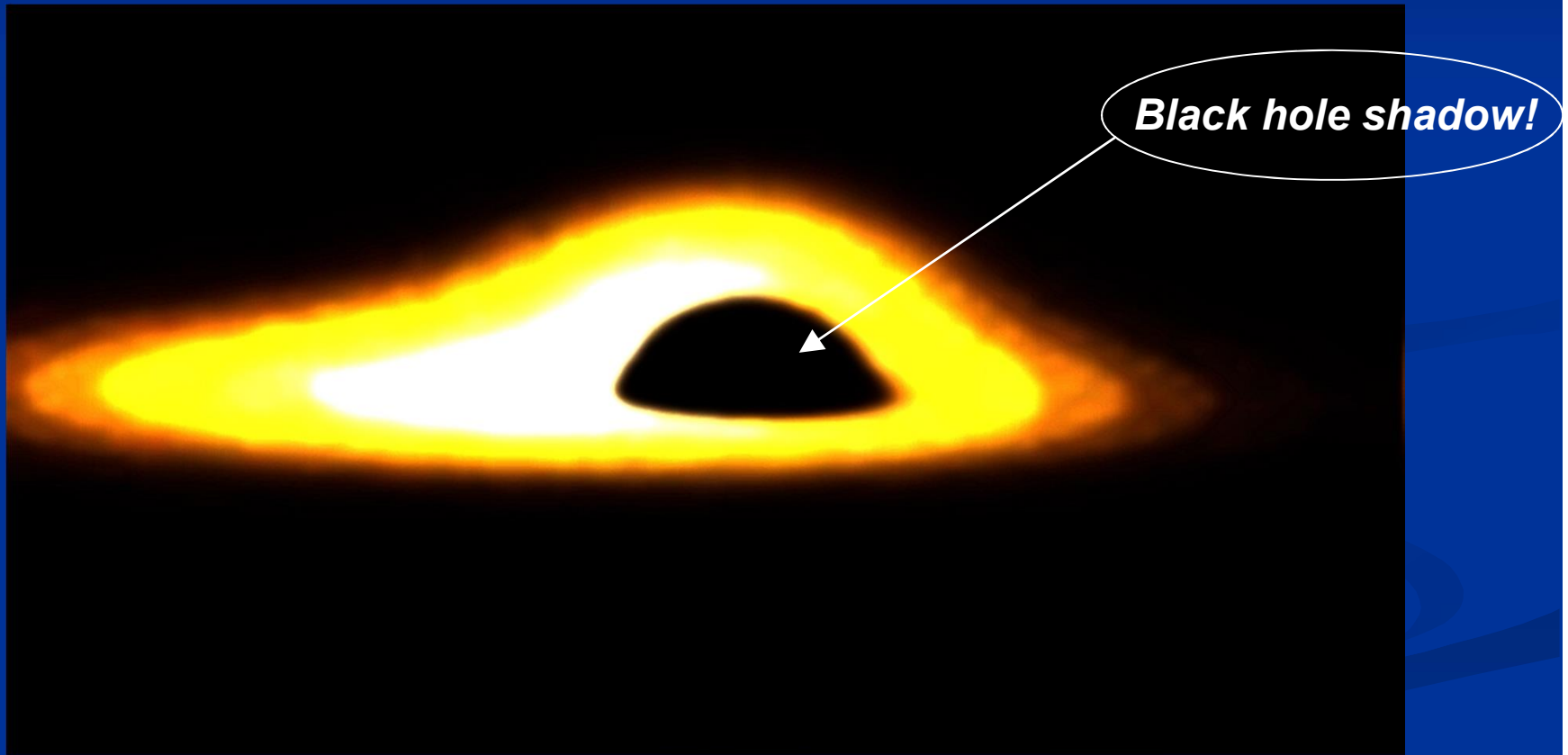
Comptonization (from thermal electrons)

Bremsstrahlung

Yuan, Quataert & Narayan 2003

Black Hole Shadow: Evidence for Strong Gravity

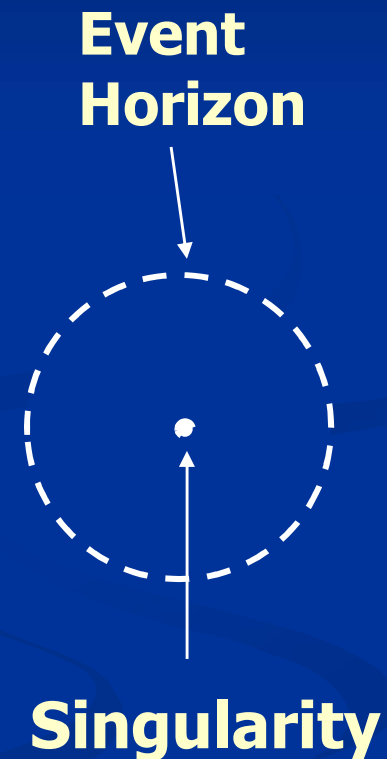
A shadow of $\sim 5R_{\text{sch}}$ size exists due to General Relativistic effect.



But this is only evidence for strong gravity: any compact objects will look same!

Evidence for Black Hole: Existence of Event Horizon

- The event horizon is a one-way membrane
- Matter/energy can fall in, but nothing gets out, not even light
- The efficiency of accretion flow in Sgr A* is very low because the gravitational energy is stored in the gas and falls on to the event horizon!
- If there were no such horizon, the stored energy would be eventually dissipated and observed!



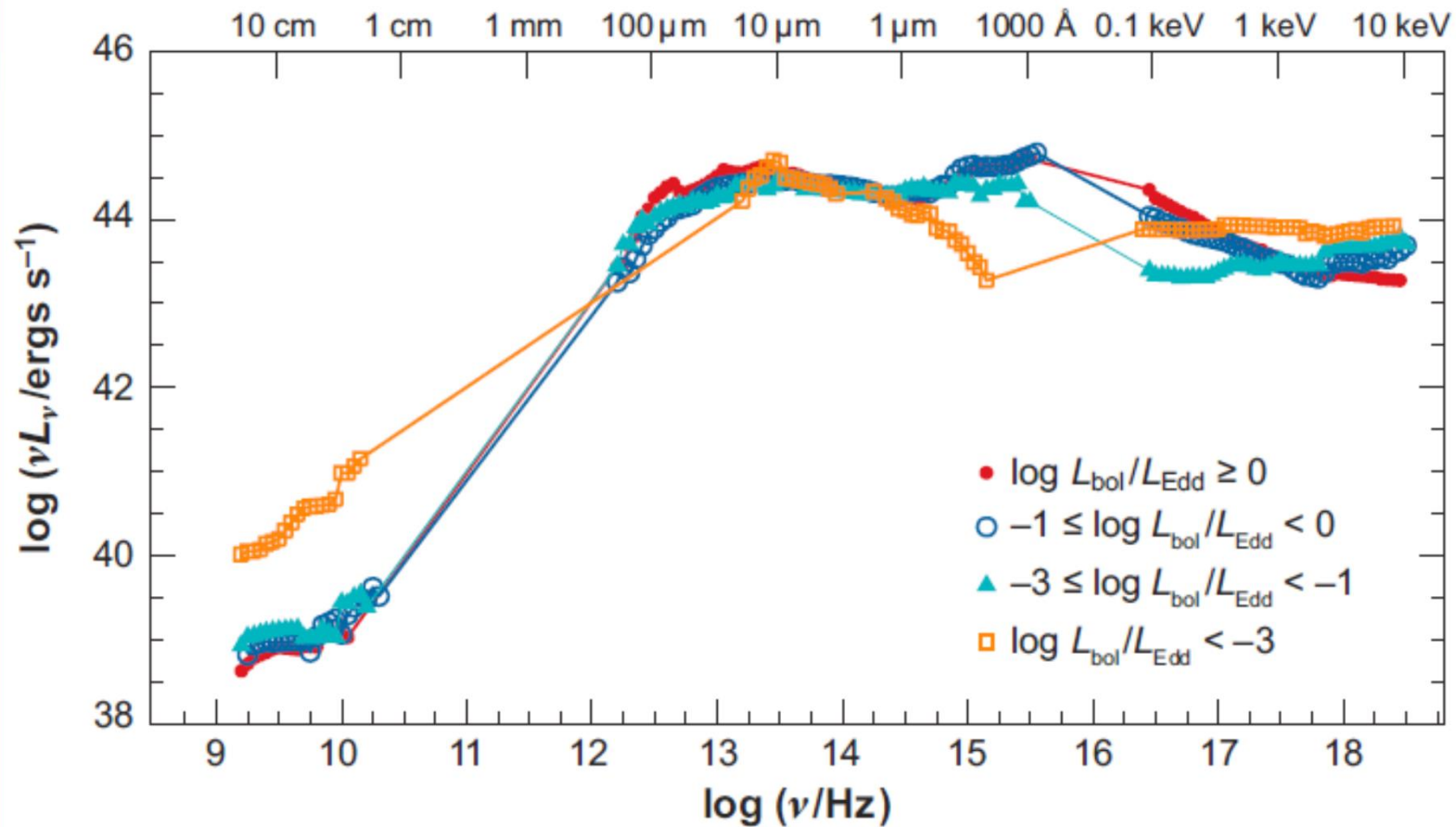
4.2: Accretion in LLAGNs

Overview of LLAGNs

Ho 1999; 2008

- 43% of nearby galaxies contain LLAGNs
- Seyferts are on average 10 times more luminous than LLAGNs
- $L_{\text{bol}}/L_{\text{Edd}} \sim 10^{-5} \text{—} 10^{-3}$
- Given the available accretion rates, the efficiency should be 1-4 orders of magnitude lower than 0.1
- Unusual SED (see next slide)
- No broad iron line
- Double-peaked iron line: $R_{\text{in}} \sim 100\text{--}1000 R_{\text{s}}$

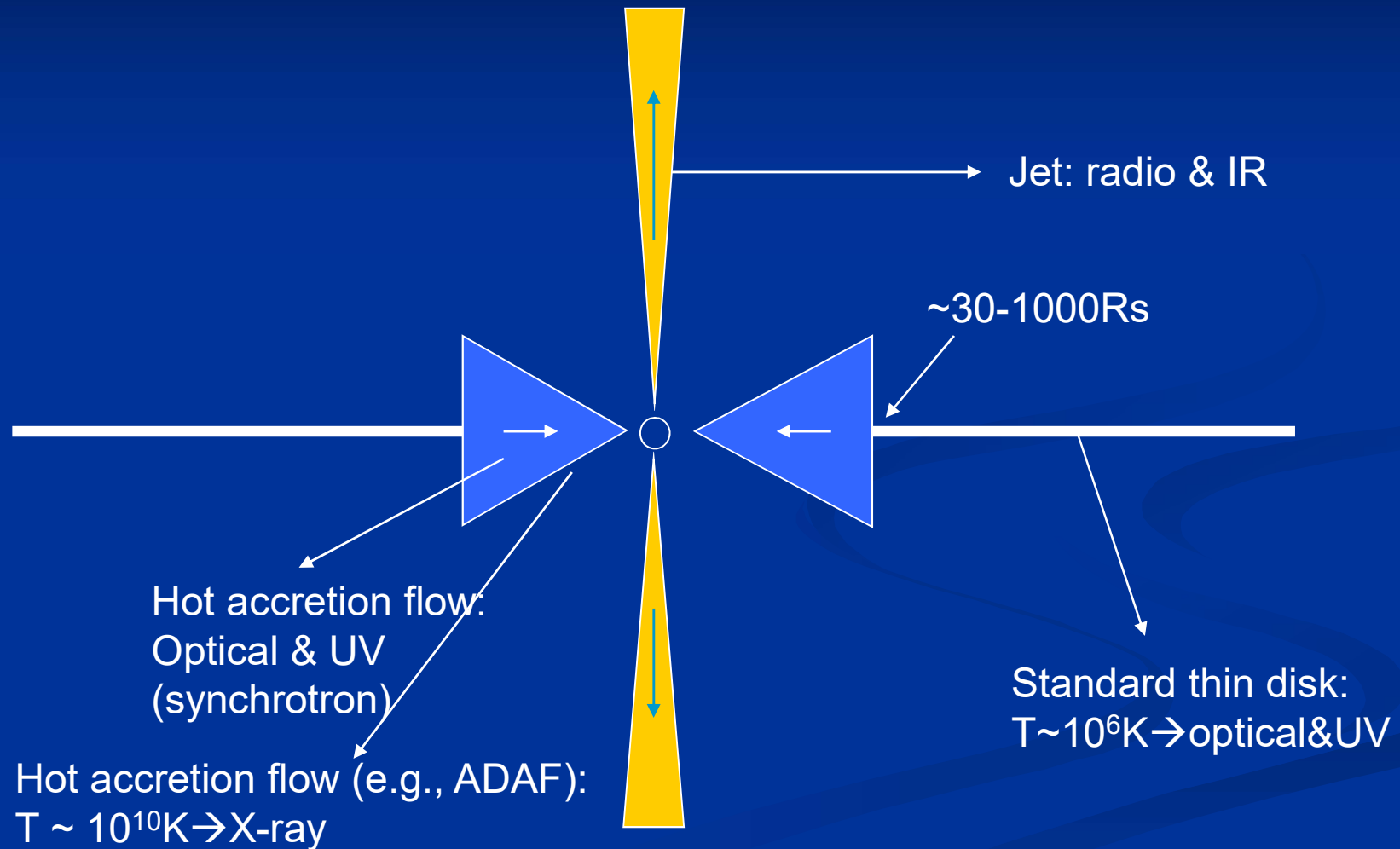
SED of LLAGNs



Ho 2008, ARA&A

Accretion geometry for LLAGNs

Esin, McClintock & Narayan 1997; Yuan, Cui & Narayan 2005



Transition radius (I): the evaporation model

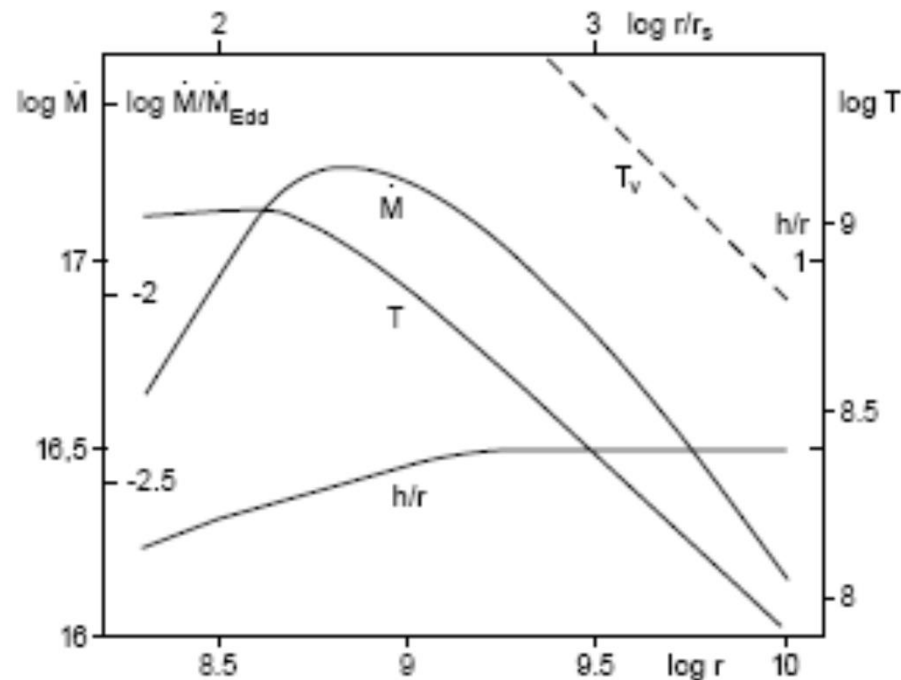


Fig. 3. Values of quantities at the inner edge $r=r_{\text{tr}}$ of the thin disk for various distances r (in cm). Rate of inward mass flow \dot{M} (in g/s) in the corona (= evaporation minus wind loss), maximum temperature in the corona and h/r (h pressure scaleheight), solid lines. Dashed line: virial temperature. Values of \dot{M} and r are for a central mass of $6M_{\odot}$, scaling with \dot{M}_{Edd} and r_s is indicated.

From Meyer, Liu & Meyer-Hofmeister 2000, A&A

Transition radius (II): turbulent energy transportation

Honma 1996, PASJ; Manmoto & Kato 2000, ApJ:

$$Q_{\text{turb}}^+ = -\frac{1}{R} \frac{d}{dR} (2RHF_{\text{turb}}), \quad (8)$$

where F_{turb} is the vertically averaged energy flux due to turbulence:

$$F_{\text{turb}} = -\rho K_T T \frac{ds}{dR} = -3(1 + \epsilon) \frac{\alpha_T \rho c_s^2}{\Omega_K} \frac{dc_s^2}{dR} + \frac{2\alpha_T c_s^4}{\Omega_K} \frac{d\rho}{dR}.$$

The above formula is similar to the convective energy flux.

Transition radius (II): turbulent energy transportation

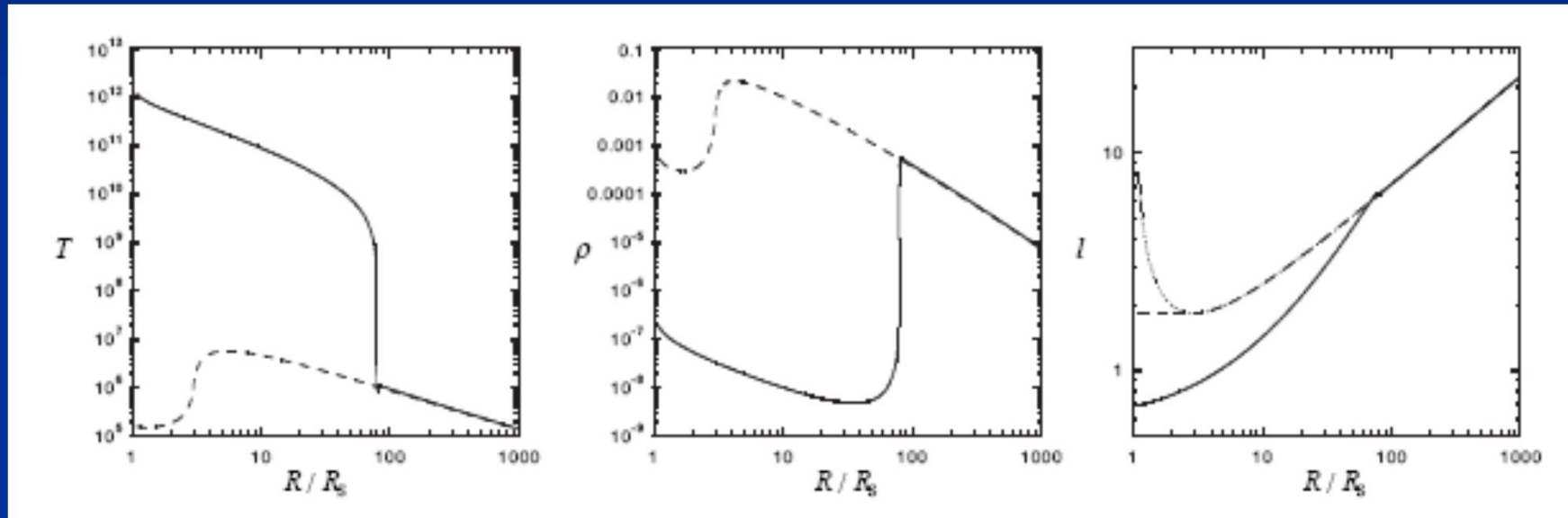
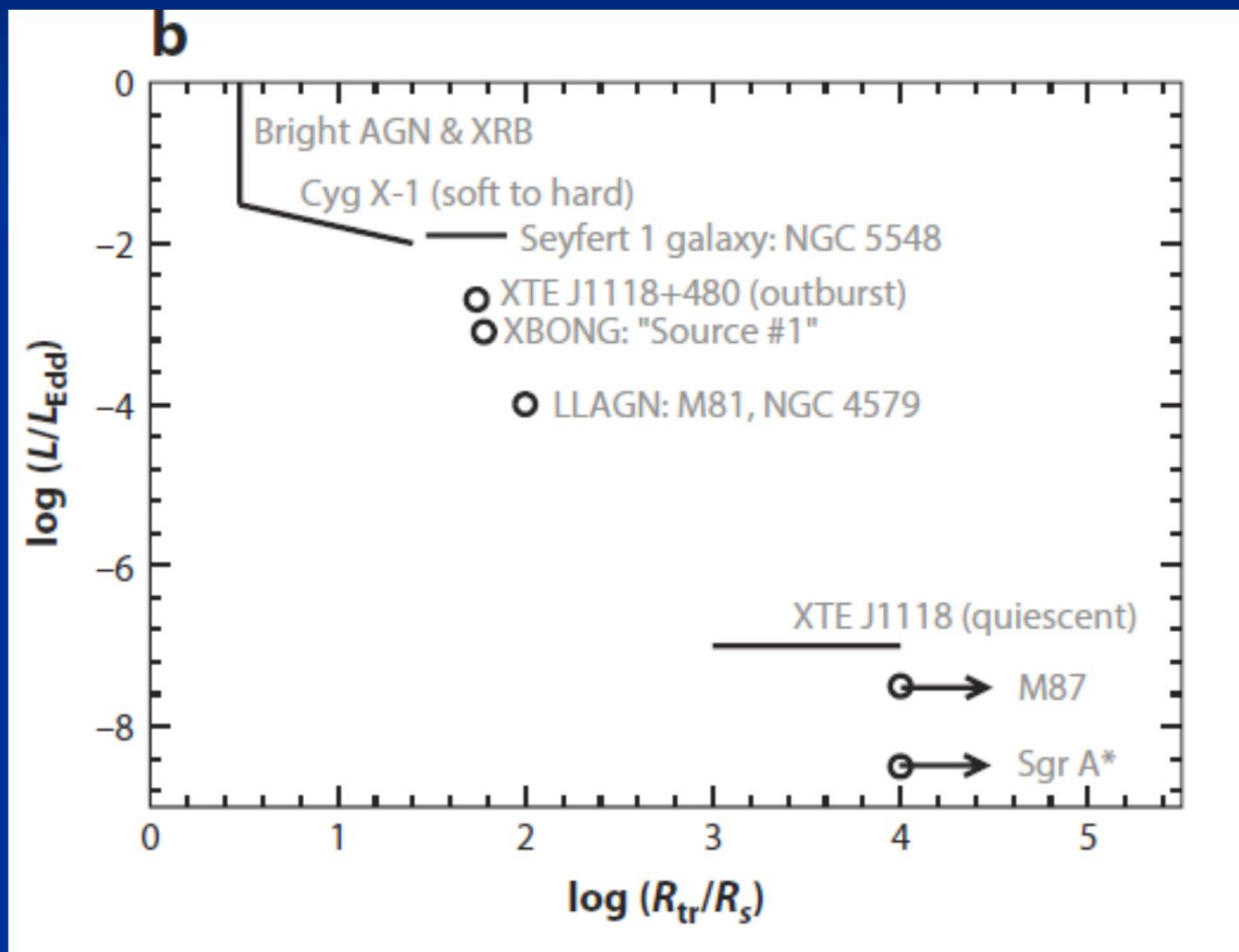


FIG. 1.—ADAF-SSD solution with $R_{tr} = 80R_S$ (solid line). The dotted lines correspond to the SSD solution. *Left:* Temperature, T . *Middle:* Density ρ . *Right:* Specific angular momentum, l , in units of cR_S . The dotted line in the right panel represents the Keplerian angular momentum.

Transition radius(III): “observation”

Yuan & Narayan 2004



M81

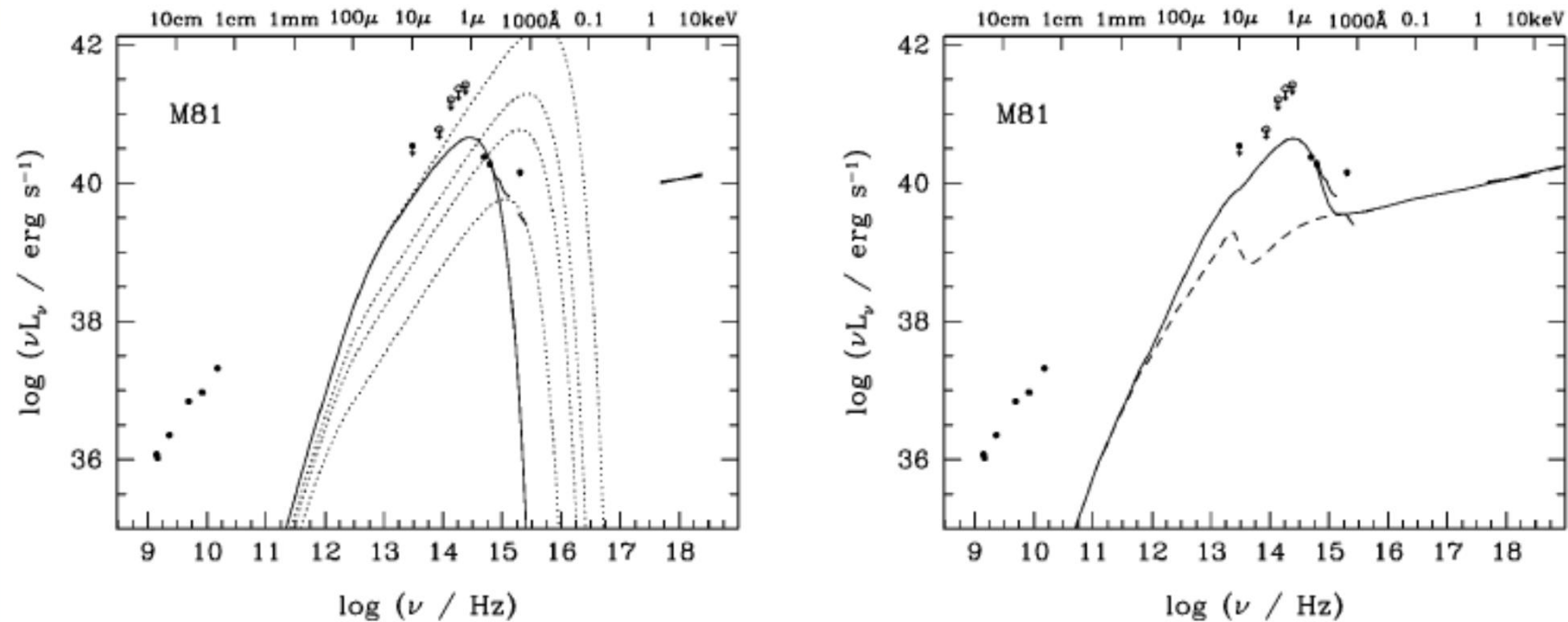


FIG. 1.—*Left:* Multicolor blackbody thin accretion disk models for the optical-UV emission from M81 (dotted lines from top to bottom: $\dot{m} = 10^{-2}$, 10^{-3} , 3×10^{-4} , and 3×10^{-5} with $r_{\text{in}} = 3$; solid line: $\dot{m} = 3 \times 10^{-3}$ and $r_{\text{in}} = 100$). *Right:* Model for M81 in which a thin disk is truncated at $r_{\text{in}} \approx 100$, inside of which there is an ADAF. The solid line shows the total "disk + ADAF" emission, while the dashed line shows the ADAF contribution. The truncated disk produces the optical/UV emission, while the X-rays are produced in the ADAF.

From Quataert et al. 1999, ApJ

NGC 4579

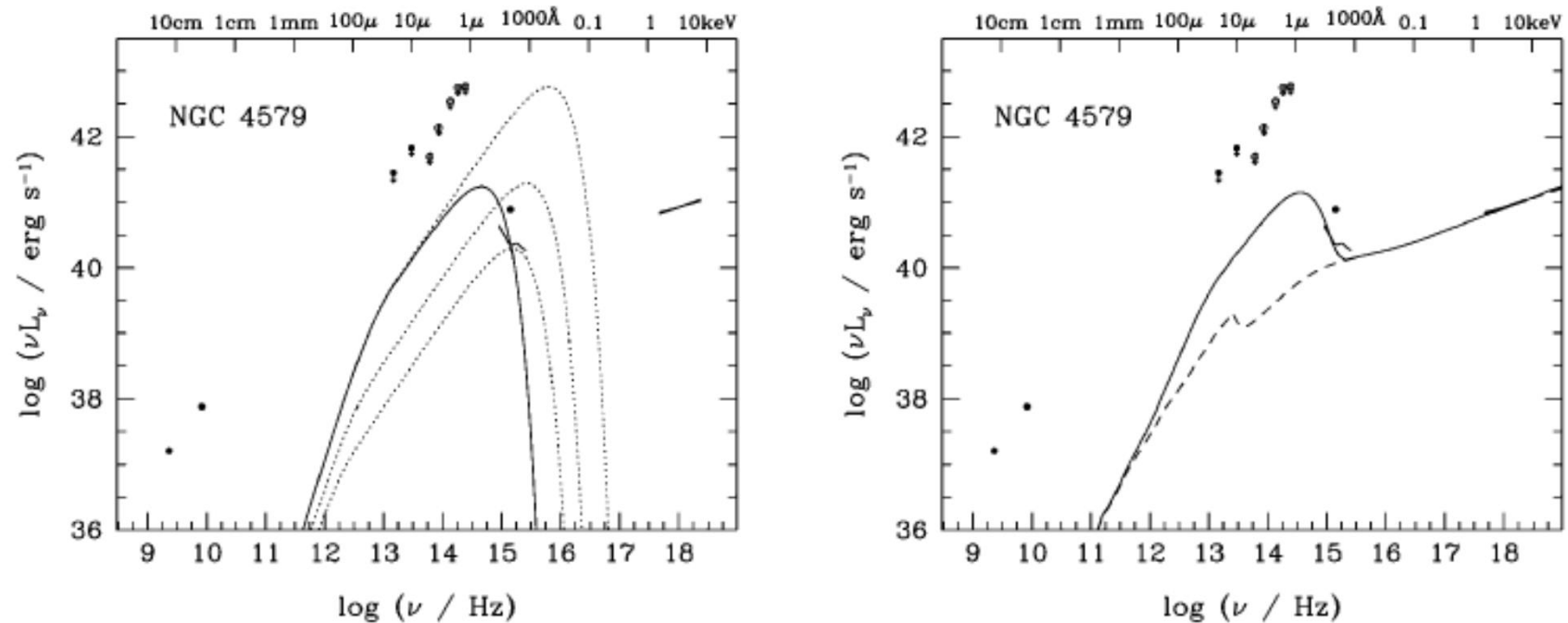


FIG. 2.—*Left:* Multicolor blackbody thin accretion disk models for the optical-UV emission from NGC 4579 (dotted lines from top to bottom: $\dot{m} = 3 \times 10^{-2}$, 10^{-3} , and 10^{-4} with $r_{\text{in}} = 3$; solid line: $\dot{m} = 0.03$ and $r_{\text{in}} = 100$). *Right:* Model for NGC 4579 in which a thin disk is truncated at $r_{\text{in}} \approx 100$, inside of which there is an ADAF. The solid line shows the total “disk + ADAF” emission, while the dashed line shows the ADAF contribution

From Quataert et al. 1999, ApJ

NGC 1097: one of the best example?

Double peaked iron line $\rightarrow R_{tr}=225$, consistent with spectral fitting result!

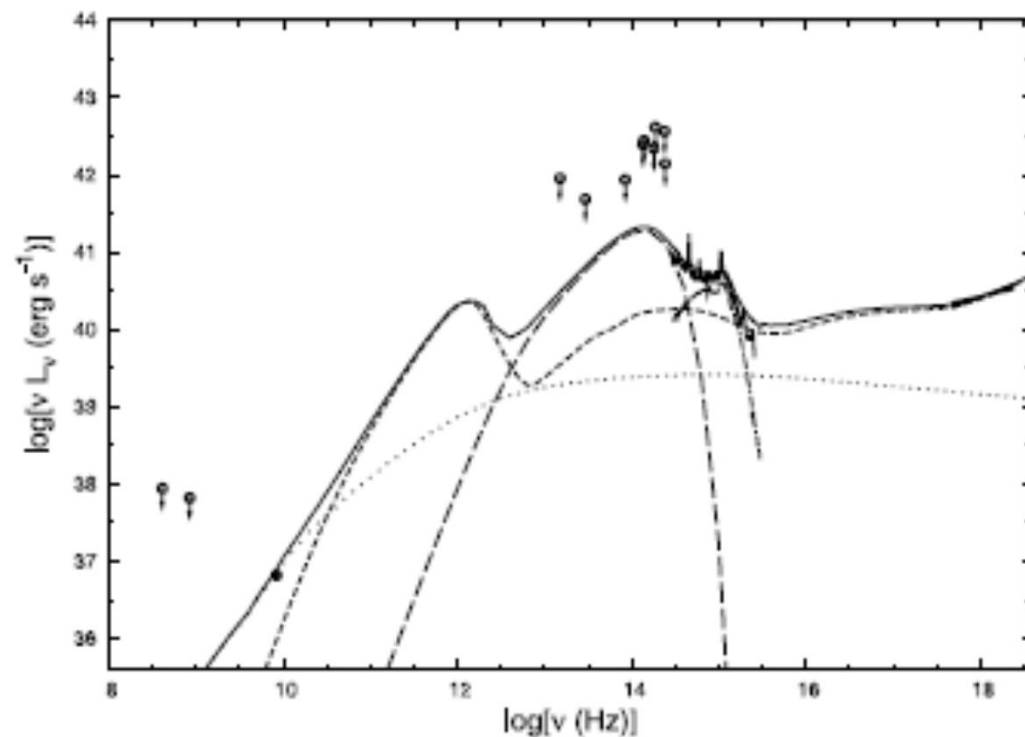


FIG. 4.—Models of the RIAF (*short-dashed line*), thin disk (*long-dashed line*), jet (*dotted line*), and obscured starburst (*dot-dashed line*) compared to the nuclear SED of NGC 1097. The sum of all components is also shown (*solid line*). The thin disk is truncated at $r_{tr} = 225$, inside of which there is a RIAF; the accretion rate decreases inward according to $\dot{m}(r) = 6.4 \times 10^{-3} (r/r_{tr})^{0.8}$ (see text). The starburst model includes the Fe II emission line.

From Nemmen et al. 2006, APJ

XBONGs

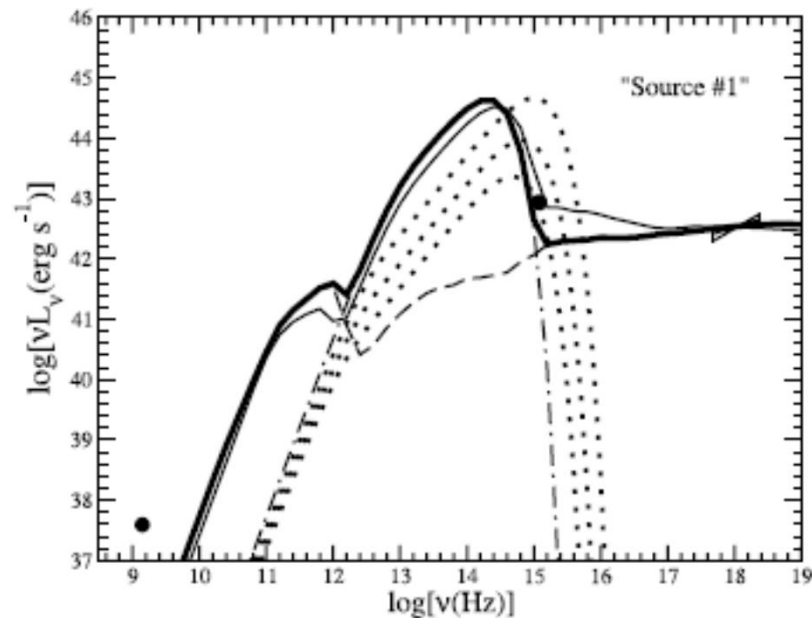


FIG. 1.—Spectral fit of the XBONG Source 1 (Severgnini et al. 2003) with an RIAF+thin disk model. The thick solid line shows the combined spectrum predicted for an accretion flow consisting of a truncated thin disk for radii $R > R_{tr} = 60R_g$ (dot-dashed line) and an RIAF for $R < R_{tr}$ (dashed line). The mass accretion rate of the RIAF at $R = R_{tr}$ is $\dot{M}_0 = 10^{-2}\dot{M}_{Edd}$, and it decreases with radius according to eq. (1) with $s = 0.3$. The thin solid line shows the result of another model (traditional ADAF), in which the accretion rate of the RIAF is taken to be independent of radius, with $\dot{M} = 10^{-2}\dot{M}_{Edd}$ and $R_{tr} = 40R_g$. The three dotted lines show the emission from three standard thin accretion disks extending all the way down to $R = 3R_g$ with (from bottom to top) $\dot{M}/\dot{M}_{Edd} = 5 \times 10^{-5}$, 2×10^{-4} , and 10^{-3} . These latter models do not fit the observations.

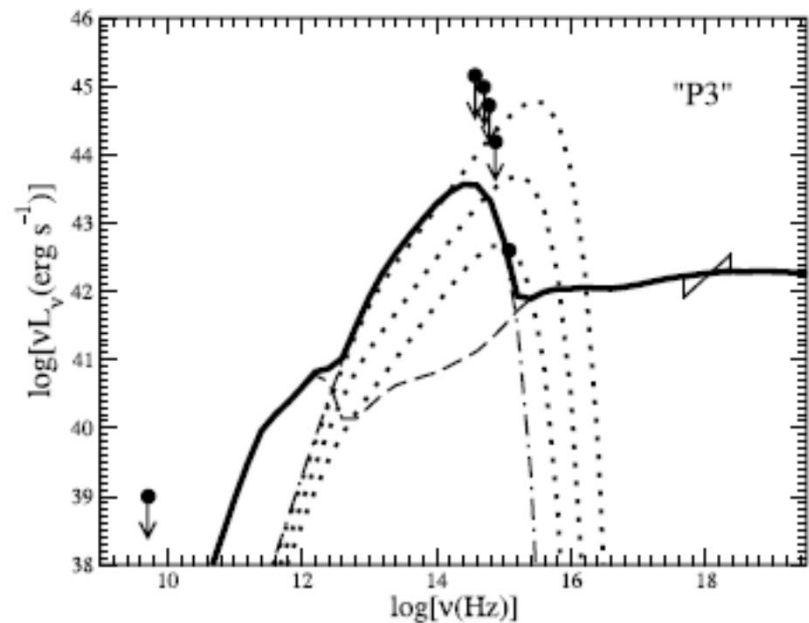


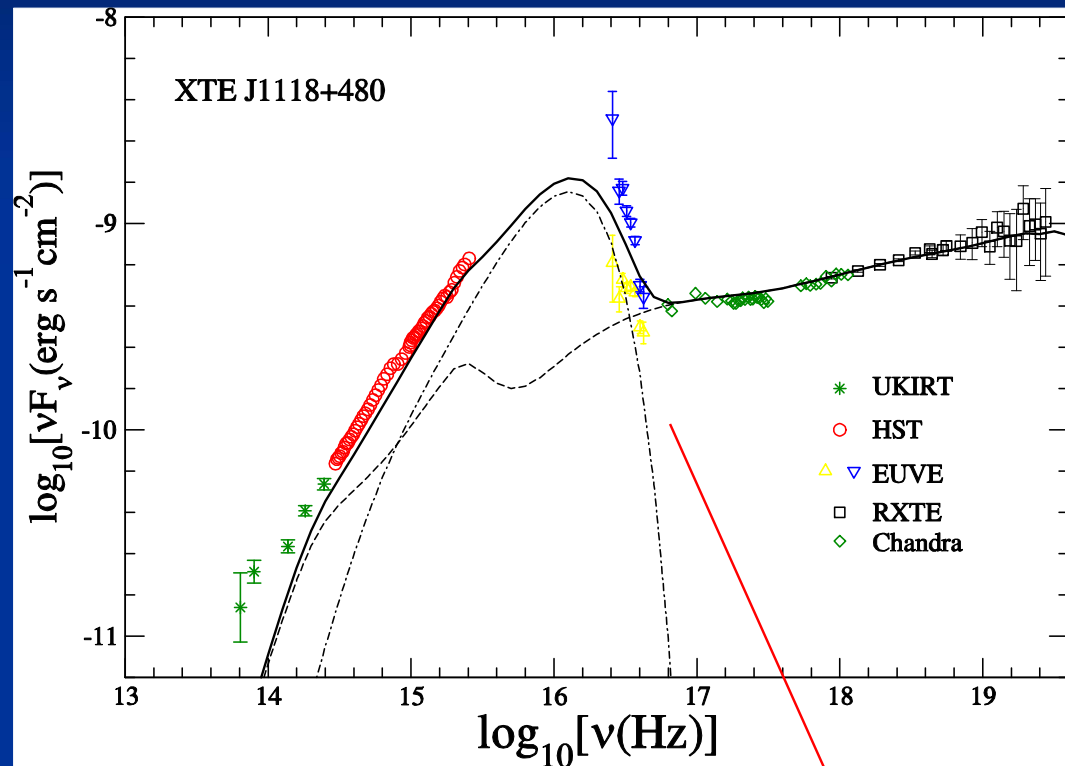
FIG. 2.—Spectral fit of the XBONG source P3 with an RIAF+thin disk model. The thick solid line shows the combined spectrum predicted for an accretion flow consisting of a truncated thin disk for radii $R > R_{tr} = 60R_g$ (dot-dashed line) and an RIAF for $R < R_{tr}$ (dashed line). The mass accretion rate of the RIAF at $R = R_{tr}$ is $\dot{M}_0 = 1.3 \times 10^{-2}\dot{M}_{Edd}$, and it decreases with radius according to eq. (1) with $s = 0.3$. The three dotted lines show the emission from three standard thin accretion disks extending all the way down to $R = 3R_g$ with (from bottom to top) $\dot{M}/\dot{M}_{Edd} = 8 \times 10^{-5}$, 8×10^{-4} , and 10^{-2} . These latter models do not fit the observations.

NGC 5548 than in LLAGNs. The thin solid line in Figure 1

The hard state of XTE J1118-480

Yuan, Cui & Narayan 2005

- $R_{\text{tr}} \sim 300 R_s$: well determined by the EUV data
- QPO of frequency 0.07---0.15 Hz is detected
- If we explain the QPO as the p-mode oscillation of the ADAF, this QPO frequency also suggests $R_{\text{tr}} \sim 300 R_s$

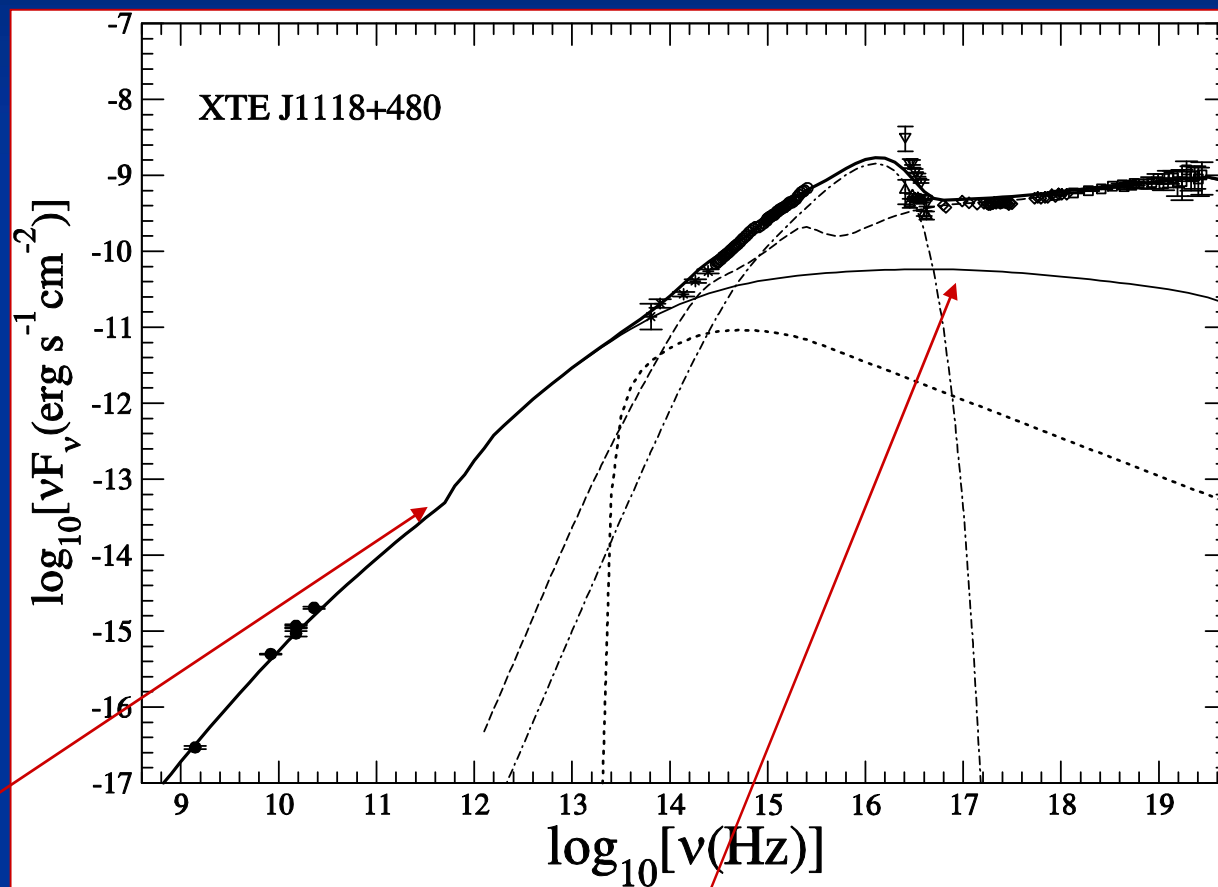


Radiation from the truncated thin disk,
with $R_{\text{tr}} = 300 R_s$

Accretion-jet model of XJTJ1118+480

Yuan, Cui & Narayan 2005

1. ~5% of the accretion material is transferred into the jet
2. Such a coupled accretion-jet system is also required to explain the complicated timing features of XTE J1118



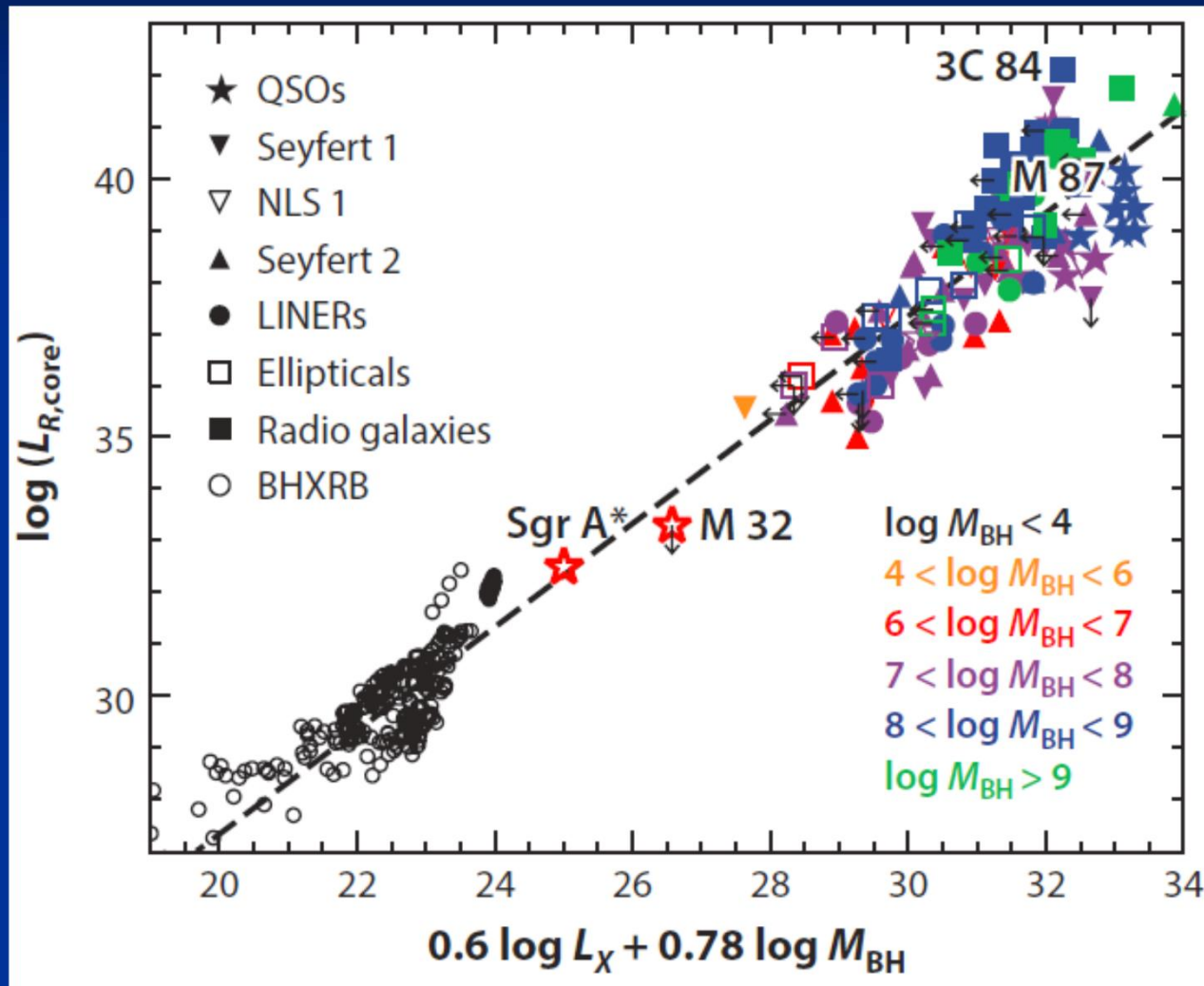
Yuan, Cui & Narayan 2005, APJ

Optically-thick synchrotron emission from the jet

Optically-thin synchrotron emission from the jet

4.3 Radio/X-ray correlation

Radio/X-ray correlation in all BHs: high-L case



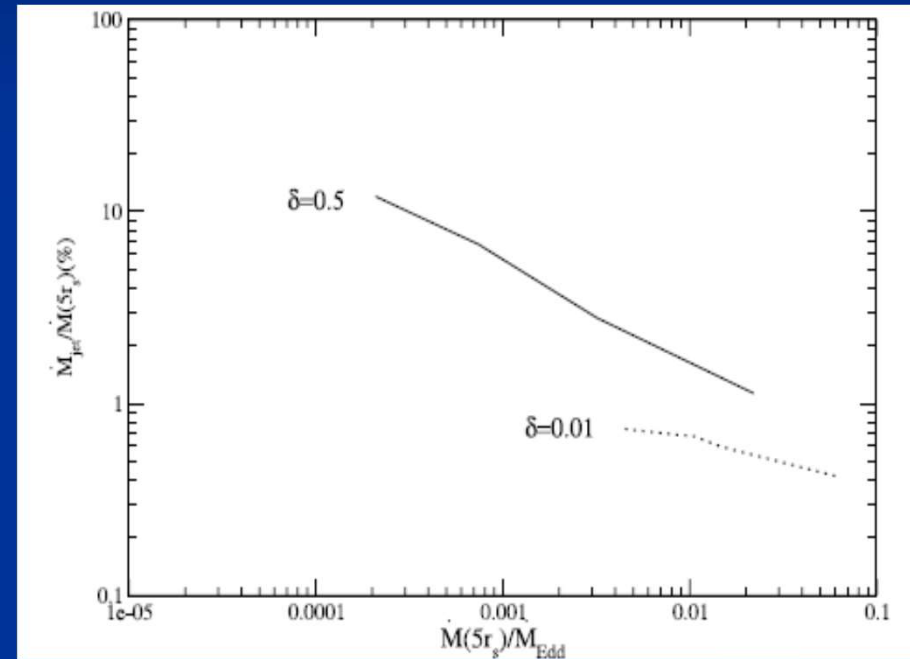
Merloni et al. 2003

$$\log L_R = (0.60^{+0.11}_{-0.11}) \log L_X + (0.78^{+0.11}_{-0.09}) \log M + 7.33^{+4.05}_{-4.07}$$

Interpretation to Merloni et al. (2003) correlation

Yuan & Cui 2005

- Radio emission:
always from jets
- X-ray emission: from
hot accretion flow
- Require: $\dot{M}_{jet}/\dot{M}_{acc}$
satisfies some relation



Prediction at lower L

(Yuan & Cui 2005)

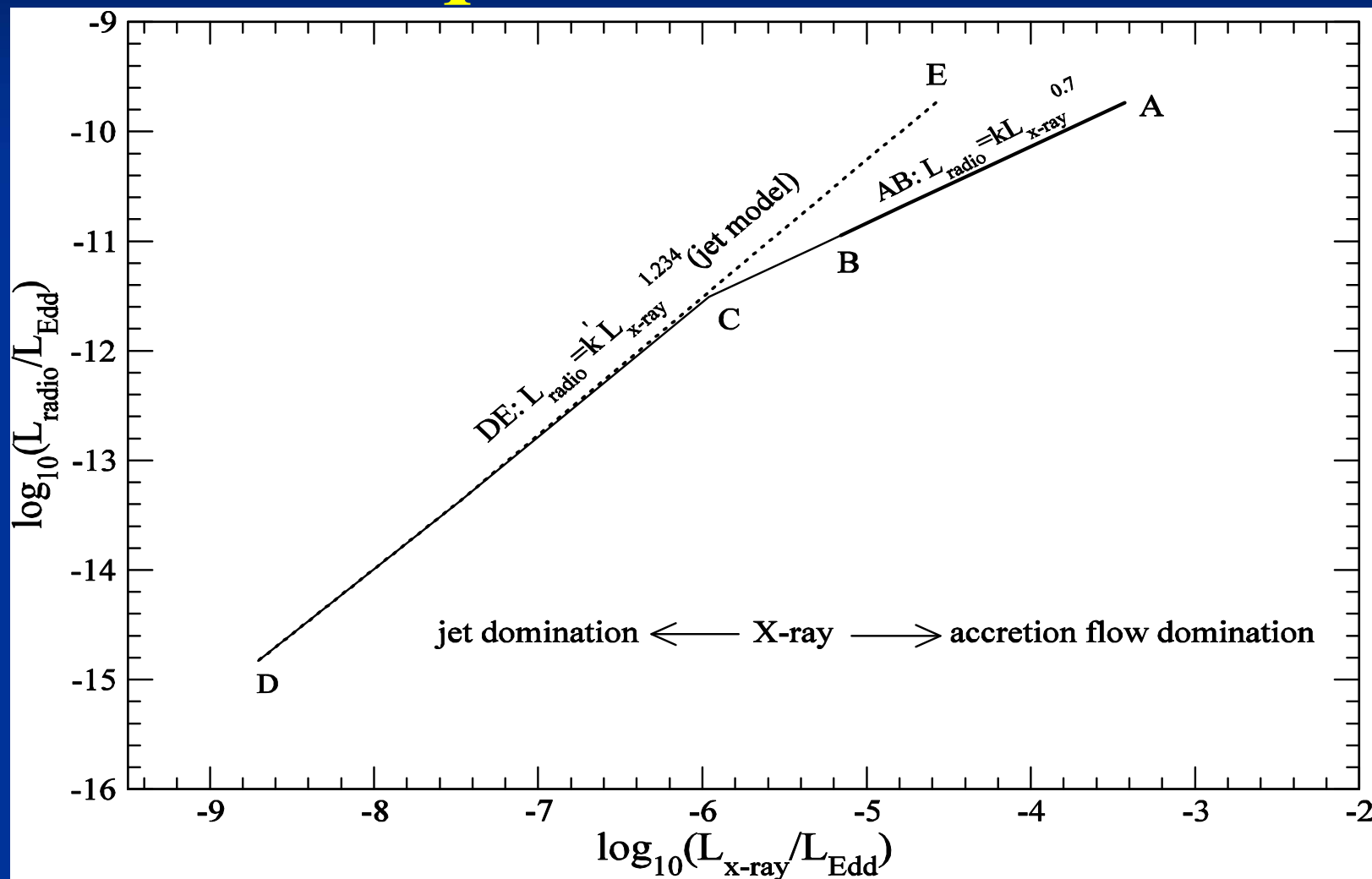
- The optically-thin synchrotron from jet $\propto \dot{M}$, while the Comptonization from the hot accretion flow $\propto \dot{M}^2$ (Heinz 2005; Yuan & Cui 2005)
- With the decrease of \dot{M} , the X-ray emission will be dominated by the jet
- Thus a change of the radio---X-ray correlation is expected

$$\log L_R = 1.23 \log L_X + 0.25 \log(M_{BH} / M_{\odot}) - 13.45$$

and the critical luminosity is:

$$\log \left(\frac{L_{X,crit}}{L_{Edd}} \right) = -5.3 - 0.17 \log \left(\frac{M}{M_{\odot}} \right)$$

Radio-X-ray correlation and the quiescent state



The change of the radio—X-ray correlation from hard to quiescent states

Observational tests of the prediction

- Jonker et al. (2004) obtained nearly simultaneous radio and X-ray fluxes of XTE J1908+094 during the decaying phase of an X-ray burst. The correlation index obtained is $1.28 \gg 0.7$
- The Chandra observation suggests that the X-ray emission of **M87** is dominated by the jet (Wilson & Yang 2002). This is because the X-ray luminosity of M87 $L_x \sim 0.8 L_{x,crit}$
- **M31** Garcia et al. (2005) detected $L_x \approx 10^{35.5} \text{ ergs}^{-1} \approx 10^{-3.5} L_{x,crit}$. They also estimated accretion rate $\dot{M}_{Bondi} \approx 6 \times 10^{-6} \dot{M}_{Edd}$. An ADAF with such a rate will underpredict the X-ray flux by 4 orders of magnitude; on the other hand, to produce such a flux with a jet, we only need:

$$\dot{M}_{jet} \approx 0.1\% \dot{M}_{Bondi}$$

Testing the prediction (II)

Wrobel et al. 2008, ApJ

PARAMETERS OF THE LLAGNs

Parameter	NGC 4621	References	NGC 4697	References
1. D (Mpc).....	18.2	1	11.7	2
2. s (pc arcsec ⁻¹).....	88	1	57	2
3. M_{\bullet} ($10^8 M_{\odot}$).....	2.7	3	1.7	2
4. $L(\text{Edd})$ (10^{46} ergs s ⁻¹).....	3.5	3	2.2	2
5. N_{H} (10^{20} cm ⁻²).....	<18.	4	<8.4	4
6. Γ	$1.8^{+0.8}_{-0.3}$	4	$1.6^{+0.5}_{-0.3}$	4
7. C -statistic per number of spectral bins.....	5/8	4	17/12	4
8. $F(2-10 \text{ keV})$ (10^{-14} ergs s ⁻¹ cm ⁻²).....	$2.1^{+1.2}_{-1.0}$	4	1.7 ± 0.7	4
9. $L(2-10 \text{ keV})$ (10^{37} ergs s ⁻¹).....	6.6	4	2.2	4
10. $L(2-10 \text{ keV})/L(\text{Edd})$ (10^{-9}).....	1.9	4	1.0	4
11. $S(8.5 \text{ GHz})$ (mJy).....	0.098 ± 0.018	4	0.092 ± 0.017	4
12. Observed $\nu L_{\nu}(8.5 \text{ GHz})$ (10^{35} ergs s ⁻¹).....	3.3	4	1.3	4
13. $\log R_{\text{X}} = \log \nu L_{\nu}(8.5 \text{ GHz})/L(2-10 \text{ keV})$	-2.3	4	-2.2	4
14. Predicted $\nu L_{\nu}(8.5 \text{ GHz})$ (10^{35} ergs s ⁻¹).....	1.5	5	3.5	5

NOTES.—Row (1): Surface brightness fluctuation distance. Row (2): Scale. Row (3): Mass of black hole. Row (4): Eddington luminosity of black hole. Row (5): Galactic plus intrinsic column density. Row (6): Photon index. Row (7): C -statistic (Cash 1979). Row (8): 2–10 keV flux. Row (9): 2–10 keV luminosity. Row (10): Eddington ratio. Row (11): 8.5 GHz flux density. Row (12): Observed radio luminosity. Row (13): Radio loudness. Row (14): Predicted radio luminosity.

REFERENCES.—(1) Ravindranath et al. 2002; (2) Pellegrini 2005; (3) Tremaine et al. 2002; (4) this work; (5) Yuan & Cui 2005.

Checking the prediction (II)

Yuan, Yu & Ho 2009

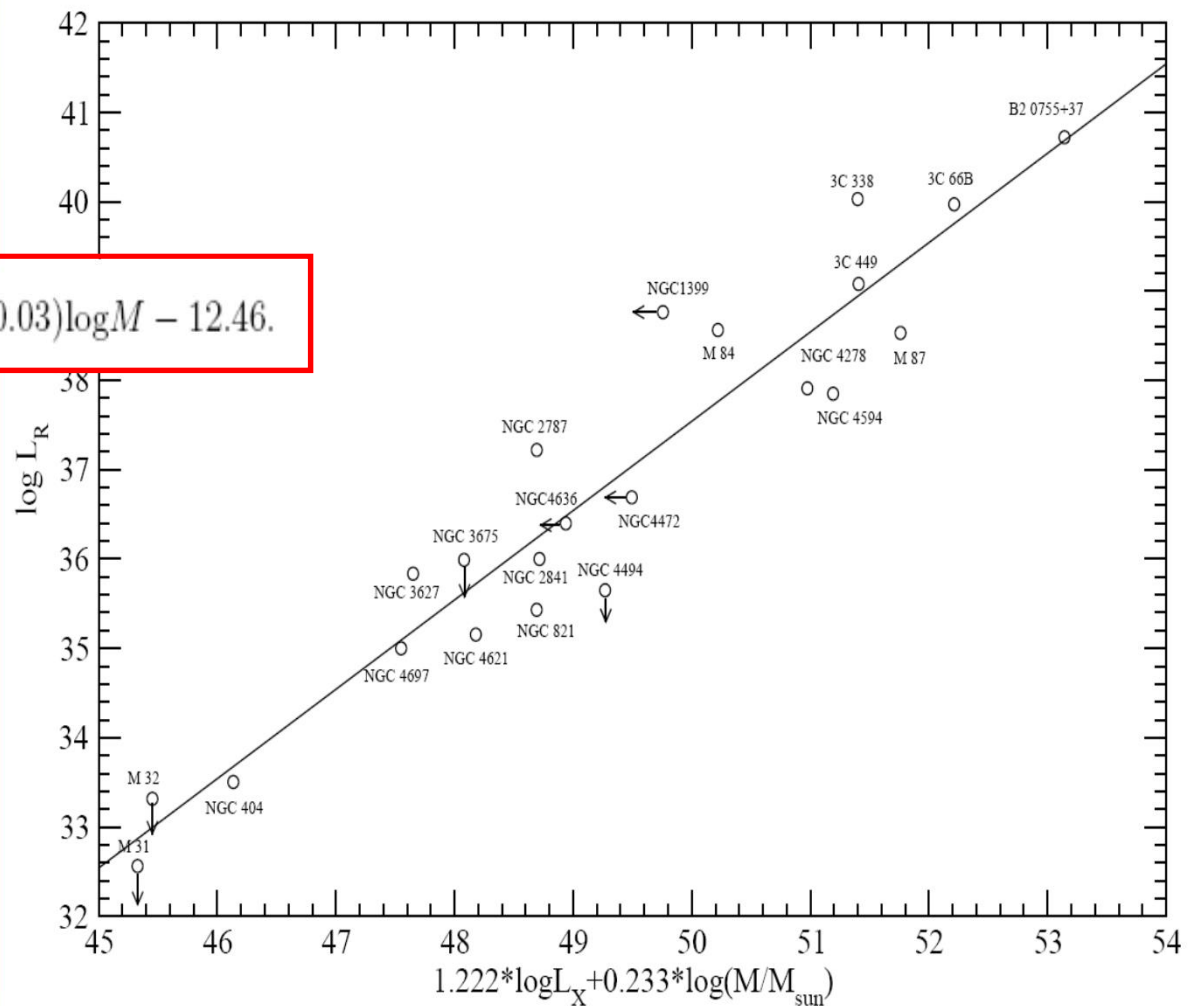
- The radio-X-ray correlation:
 - We collect radio and X-ray data for sources with $L_X < L_{X,\text{crit}}$ and see their correlation
- The X-ray spectra:
 - We model the sources with good X-ray spectral data and $L_X < L_{X,\text{crit}}$, to see the spectrum can be fitted by jet or ADAF.

Checking the correlation

- For all the 22 sources, the best correlation is

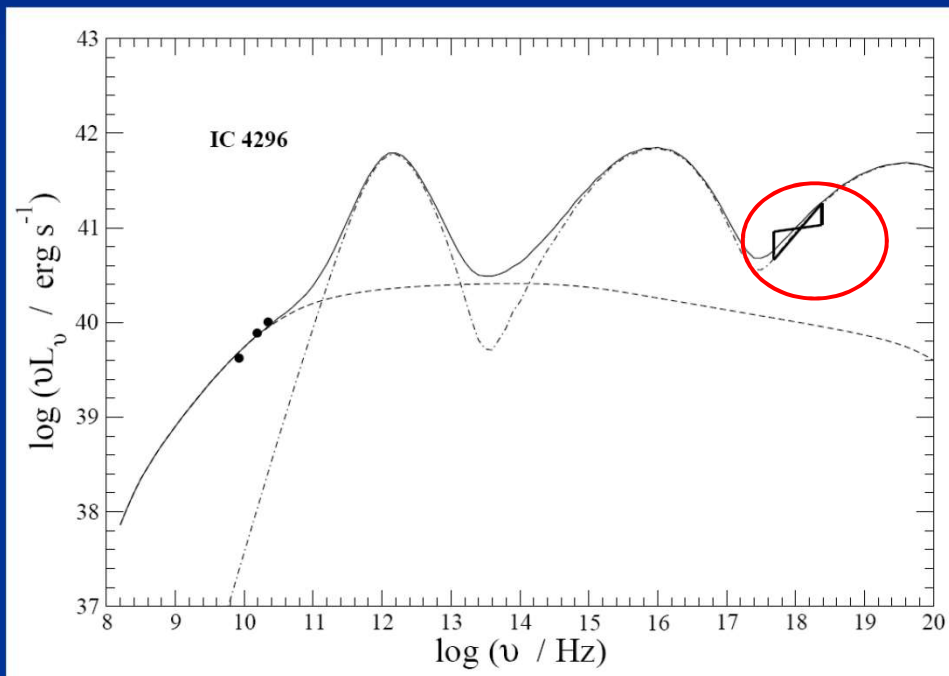
$$\log L_R = 1.22(\pm 0.02)\log L_X + 0.23(\pm 0.03)\log M - 12.46.$$

Yuan, Yu & Ho 2009

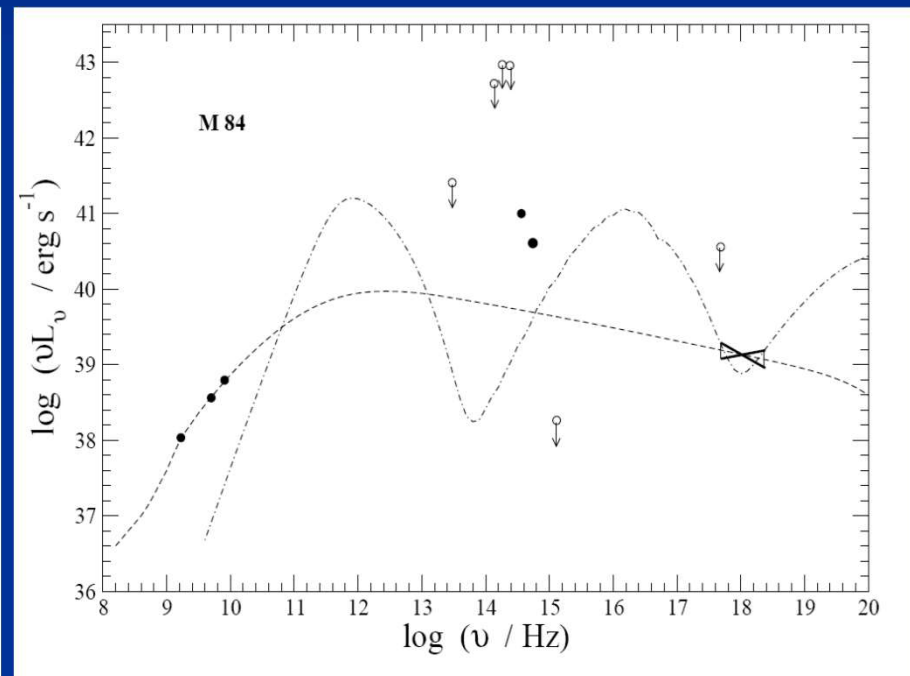


Checking the spectrum

Yuan, Yu & Ho 2009



ADAF-dominated case



Jet-dominated case